

The Generalized Polarizabilities of the proton

Nikos Sparveris



The 33rd Winter Workshop on Nuclear Dynamics
Utah, January 2017

Supported by the DOE / NP award DE-SC0016577 and the NSF / PHY award 1305536

Proton Polarizabilities

Fundamental structure constants
(such as mass, size, shape, ...)

Response of internal structure
& dynamics to external EM field

Sensitive to the full excitation
spectrum of the nucleon (contrary
to the elastic FFs)

Accessed experimentally through
Compton Scattering processes

Virtual Compton Scattering:

Virtuality of photon gives access to the
Generalized Polarizabilities $\alpha_E(Q^2)$ & $\beta_M(Q^2)$

→ mapping out the spatial distribution of
the polarization densities

Fourier transform of densities of electric charges and
magnetization of a nucleon deformed by an applied EM field

PDG

150 Baryon Summary Table

N BARYONS
 $(S = 0, I = 1/2)$

$p, N^+ = uud; \quad n, N^0 = udd$

P

$$I(J^P) = \frac{1}{2}(\frac{1}{2}^+)$$

Mass $m = 1.00727646681 \pm 0.00000000009$ u

Mass $m = 938.272046 \pm 0.000021$ MeV [a]

$|m_p - m_{\bar{p}}|/m_p < 7 \times 10^{-10}$, CL = 90% [b]

$|\frac{q_p}{m_p}|/(\frac{q_{\bar{p}}}{m_{\bar{p}}}) = 0.9999999991 \pm 0.0000000009$

$|q_p + q_{\bar{p}}|/e < 7 \times 10^{-10}$, CL = 90% [b]

$|q_p + q_e|/e < 1 \times 10^{-21}$ [c]

Magnetic moment $\mu = 2.792847356 \pm 0.000000023 \mu_N$

$(\mu_p + \mu_{\bar{p}})/\mu_p = (0 \pm 5) \times 10^{-6}$

Electric dipole moment $d < 0.54 \times 10^{-23}$ e cm

Electric polarizability $\alpha = (11.2 \pm 0.4) \times 10^{-4} \text{ fm}^3$

Magnetic polarizability $\beta = (2.5 \pm 0.4) \times 10^{-4} \text{ fm}^3$ (S = 1.2)

Charge radius, μp Lamb shift = 0.84087 ± 0.00039 fm [d]

Charge radius, $e p$ CODATA value = 0.8775 ± 0.0051 fm [d]

Magnetic radius = 0.777 ± 0.016 fm

Mean life $\tau > 2.1 \times 10^{29}$ years, CL = 90% [e] ($p \rightarrow$ invisible mode)

Mean life $\tau > 10^{31}$ to 10^{33} years [e] (mode dependent)

Physical content of the nucleon polarizabilities

Coupling of the electric and magnetic fields of a photon with the internal structure of the nucleon

When expanding the RCS amplitude in the energy of the photon:

0th and 1st order terms are expressed in terms of the charge, mass, & the anomalous magnetic moment of the nucleon

2nd order terms describe the response of the nucleon's internal structure to an electric or a magnetic dipole field

$$H_{\text{eff}}^{(2)} = -4\pi \left[\frac{1}{2} \alpha_{E1} \mathbf{E}^2 + \frac{1}{2} \beta_{M1} \mathbf{H}^2 \right]$$

The proportionality coefficients are the electric α_E & the magnetic scalar dipole polarizabilities β_M

$$\alpha_{E1}^p = 12.1 \pm 0.3 \text{ (stat.)} \mp 0.4 \text{ (syst.)} \pm 0.3 \text{ (mod.)}$$

$$\beta_{M1}^p = 1.6 \pm 0.4 \text{ (stat.)} \pm 0.4 \text{ (syst.)} \pm 0.4 \text{ (mod.)}.$$

3rd order terms: internal spin structure of the nucleon

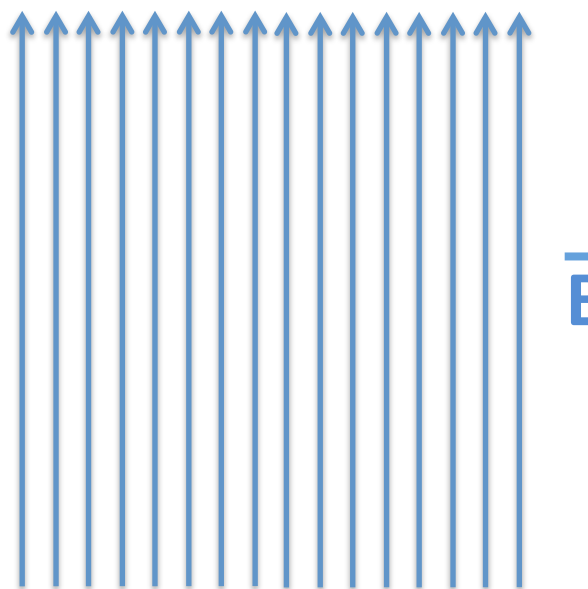
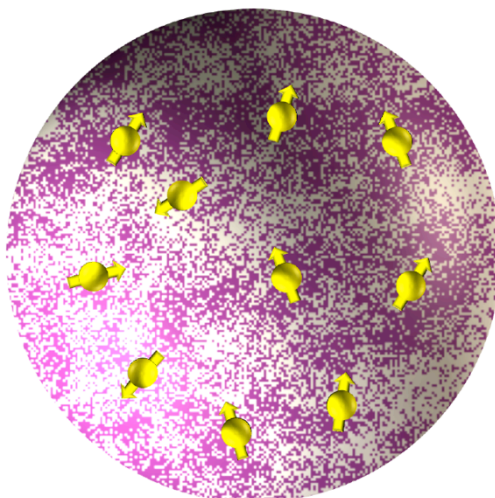
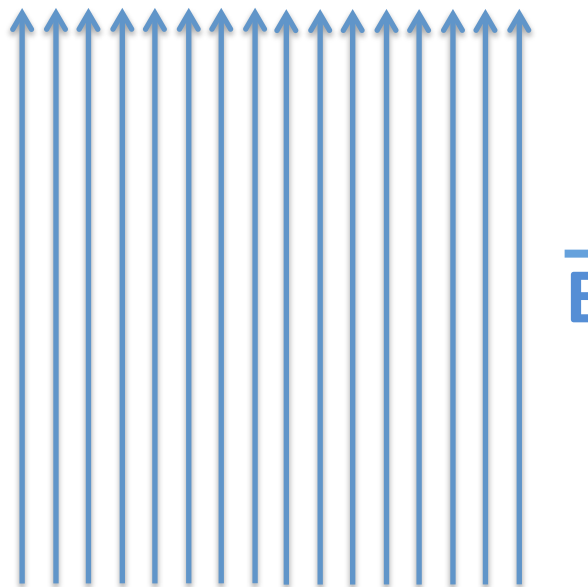
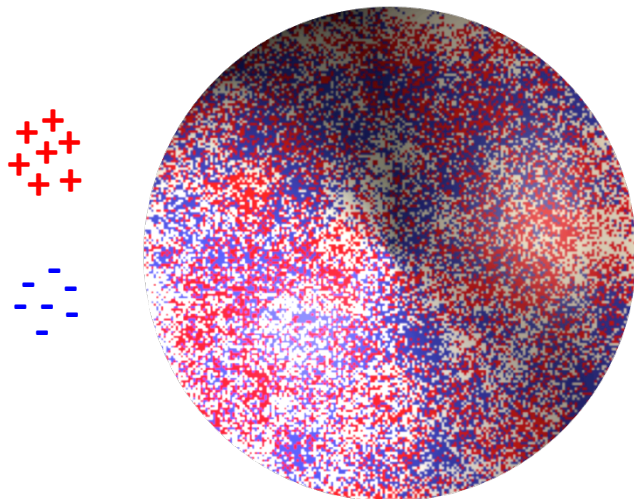
$$H_{\text{eff}}^{(3)} = -4\pi \left[\frac{1}{2} \gamma_{E1E1} \boldsymbol{\sigma} \cdot (\mathbf{E} \times \dot{\mathbf{E}}) + \frac{1}{2} \gamma_{M1M1} \boldsymbol{\sigma} \cdot (\mathbf{H} \times \dot{\mathbf{H}}) \right. \\ \left. - \gamma_{M1E2} E_{ij} \boldsymbol{\sigma}_i H_j + \gamma_{E1M2} H_{ij} \boldsymbol{\sigma}_i E_j \right],$$

$$\dot{\mathbf{E}} = \partial_t \mathbf{E}$$

$$E_{ij} = \frac{1}{2}(\nabla_i E_j + \nabla_j E_i)$$

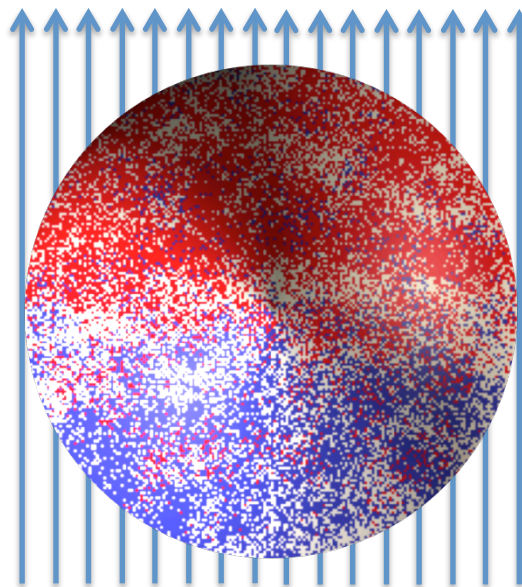
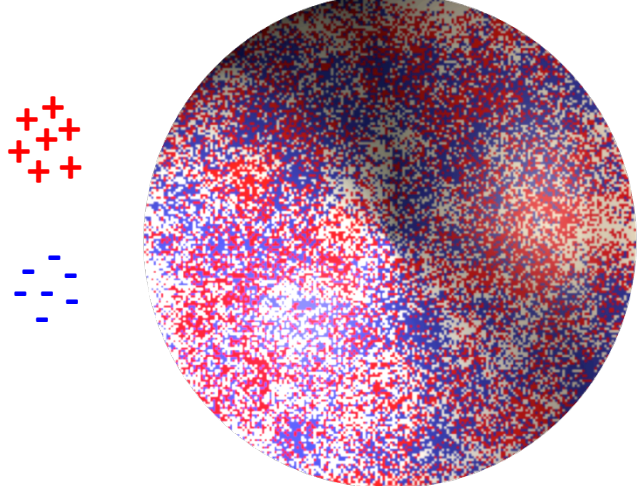
Scalar Polarizabilities

Response of internal structure to an applied EM field



Scalar Polarizabilities

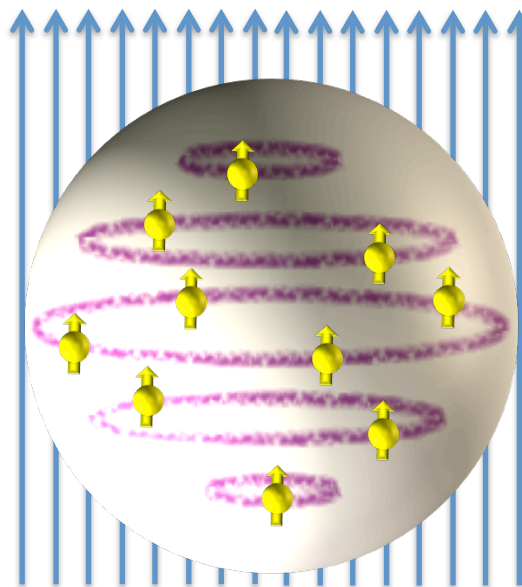
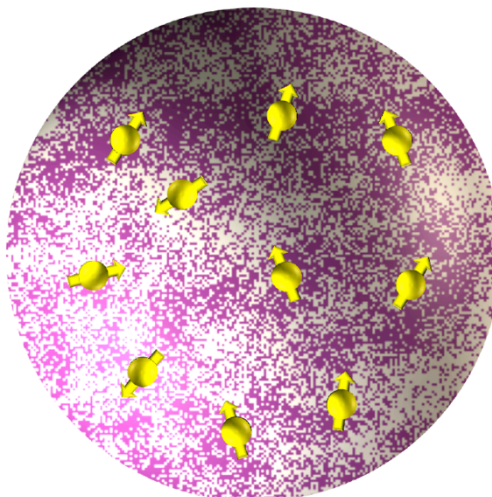
Response of internal structure to an applied EM field



“stretchability”

$$\vec{d}_{\text{E induced}} \sim \alpha \vec{E}$$

External field deforms
the charge distribution



“alignability”

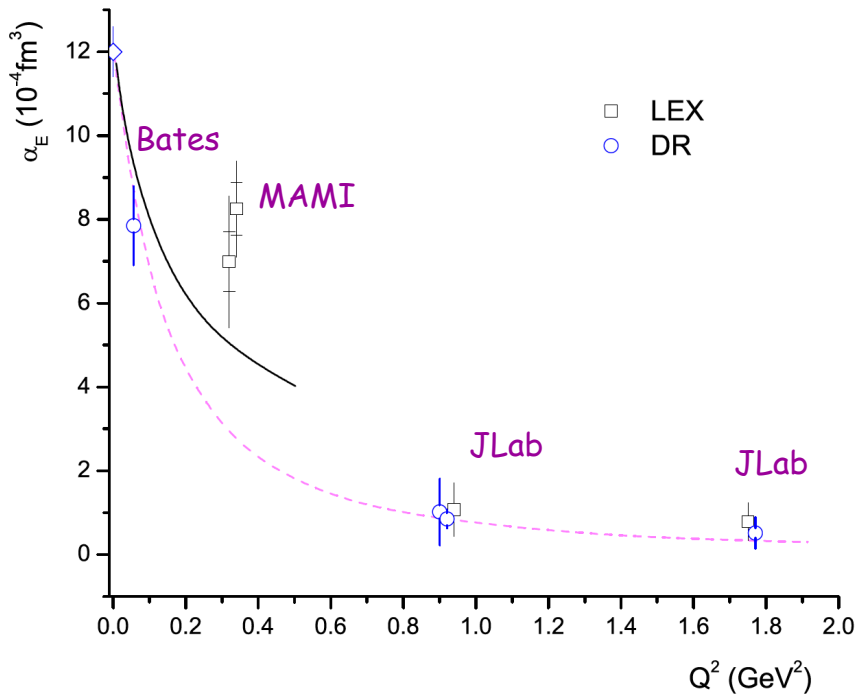
$$\vec{d}_{\text{M induced}} \sim \beta \vec{B}$$

$$\begin{aligned}\beta_{\text{para}} &> 0 \\ \beta_{\text{diam}} &< 0\end{aligned}$$

Paramagnetic: proton spin aligns
with the external magnetic field

Diamagnetic: π -cloud induction produces
field counter to the external one

Experimental Landscape



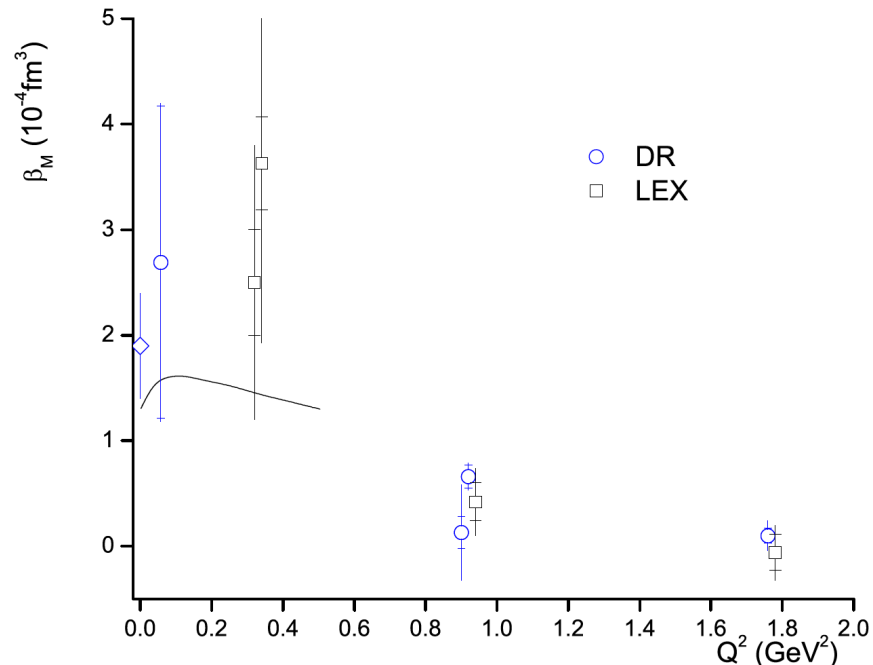
$\alpha_E \approx 10^{-3} V_N$ (stiffness / relativistic character)

Data suggest non-trivial Q^2 evolution of α_E

Current theoretical calculations not able to describe the enhancement at low Q^2

$Q^2 = 0.33 (\text{GeV}/c)^2$ measured twice at MAMI:

- Phys. Rev. Lett 85, 708 (2000)
- Eur. Phys. J. A37, 1-8 (2008)



β_M small \leftrightarrow cancellation of competing mechanisms

Large uncertainties

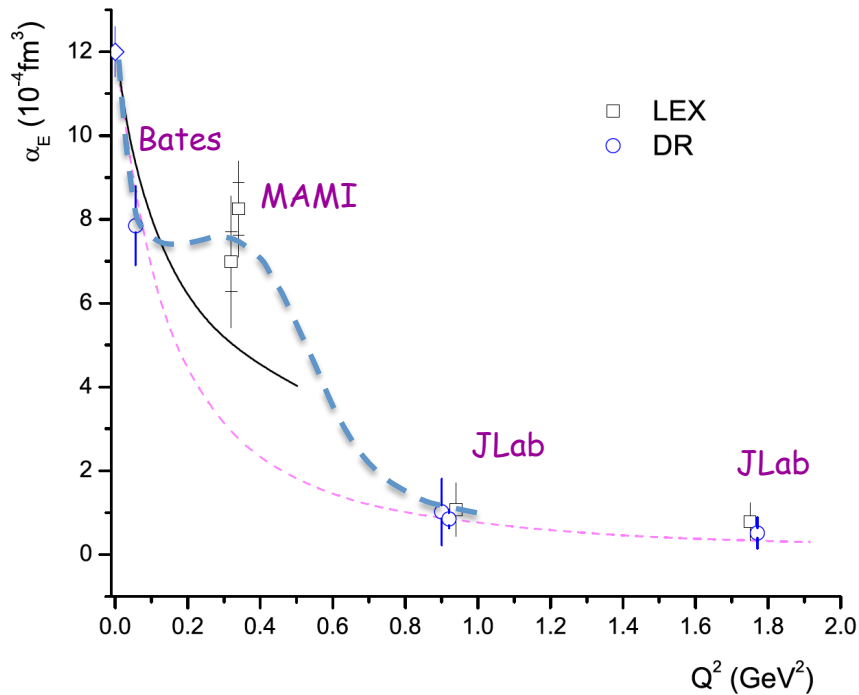
Higher precision measurements needed

\rightarrow Quantify the balance between diamagnetism and paramagnetism

Current situation unsatisfactory:

- more measurements needed (vs Q^2)
- Higher precision measurements needed

Experimental Landscape



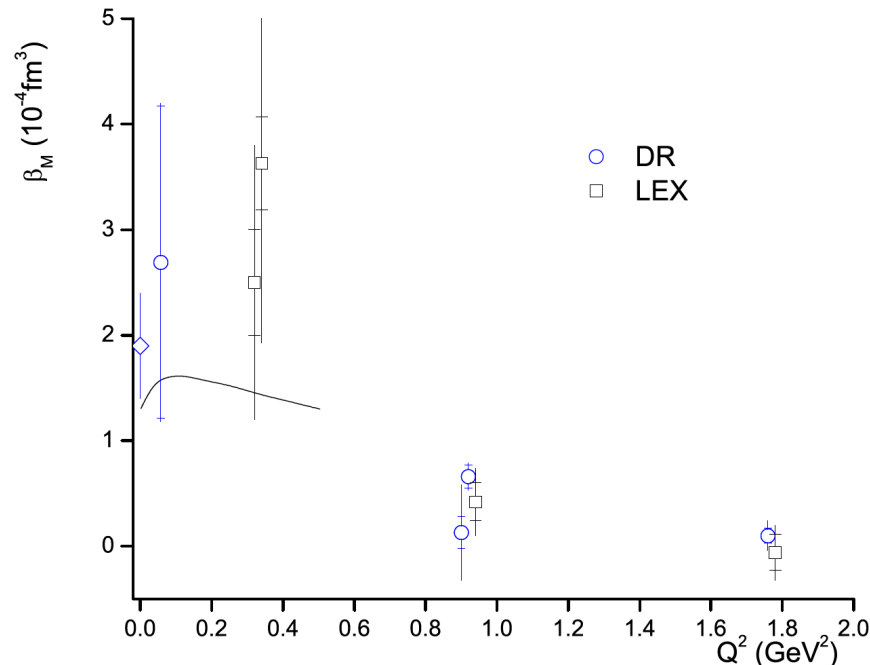
$\alpha_E \approx 10^{-3} V_N$ (stiffness / relativistic character)

Data suggest non-trivial Q^2 evolution of α_E

Current theoretical calculations not able to describe the enhancement at low Q^2

$Q^2 = 0.33 (\text{GeV}/c)^2$ measured twice at MAMI:

- Phys. Rev. Lett 85, 708 (2000)
- Eur. Phys. J. A37, 1-8 (2008)



β_M small \leftrightarrow cancellation of competing mechanisms

Large uncertainties

Higher precision measurements needed

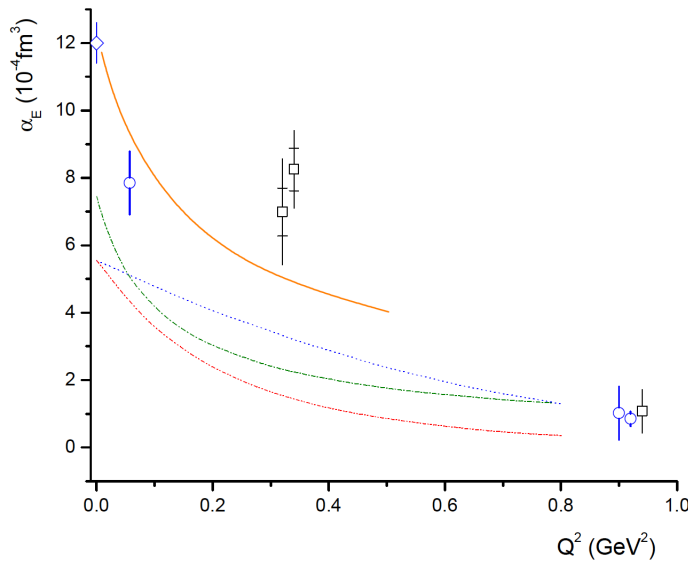
\rightarrow Quantify the balance between diamagnetism and paramagnetism

Current situation unsatisfactory:

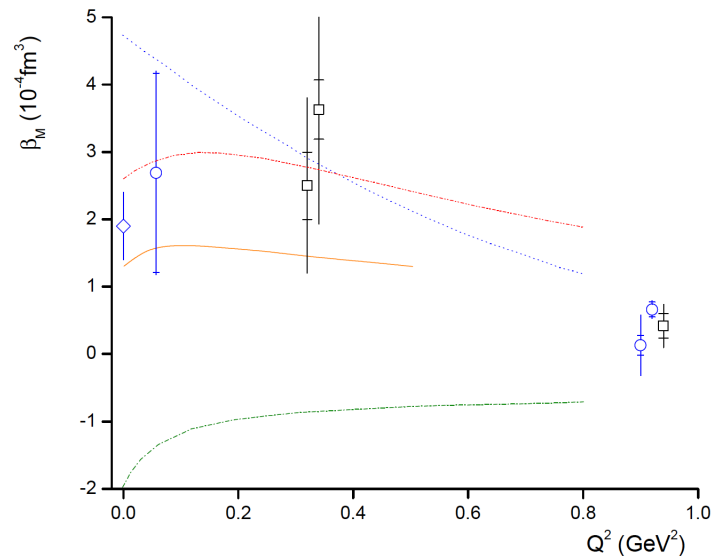
- more measurements needed (vs Q^2)
- Higher precision measurements needed

Theoretical Landscape

HBChPT
 NRQCM
 Effective Lagrangian Model
 Linear Sigma Model



T.R. Hemmert et al	Phys. Rev. D 62, 014013 (2000)
B. Pasquini et al	Phys. Rev. C 63, 025205 (2001)
A. Yu. Korchin and O. Scholten	Phys. Rev. C 58, 1098 (1998)
A. Metz and D. Drechsel	Z. Phys. A 356, 351 (1996)



All theoretical calculations predict a smooth fall off for α_E

None of the models can account for the non trivial structure of α_E suggested by the data

Lattice QCD

Currently:

Near Future:

$Q^2=0$ calculations exist but at unphysical quark masses
 calculations at the physical point for $Q^2=0$
 first calculations for $Q^2 \neq 0$

Spatial dependence of induced polarizations in an external EM field

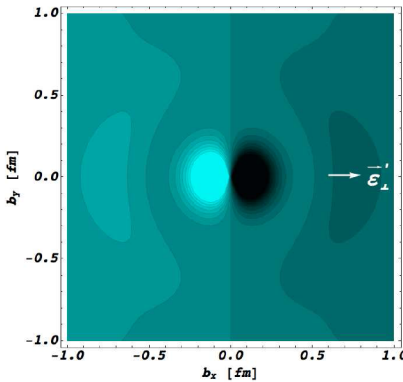
Nucleon form factor data → light-front quark charge densities

Formalism extended to the deformation of these quark densities when applying an external e.m. field:

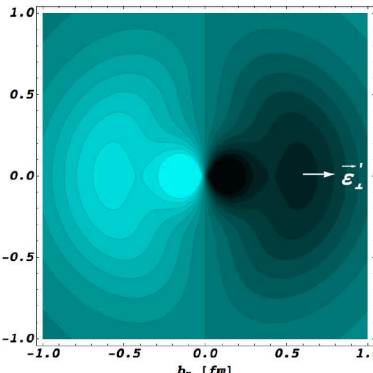
GPs → spatial deformation of charge & magnetization densities under an applied e.m. field

Induced polarization in a proton when submitted to an e.m. field

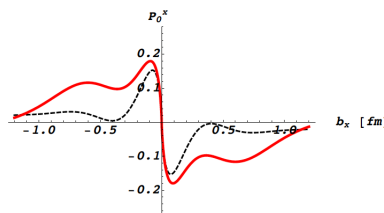
GP I



GP II



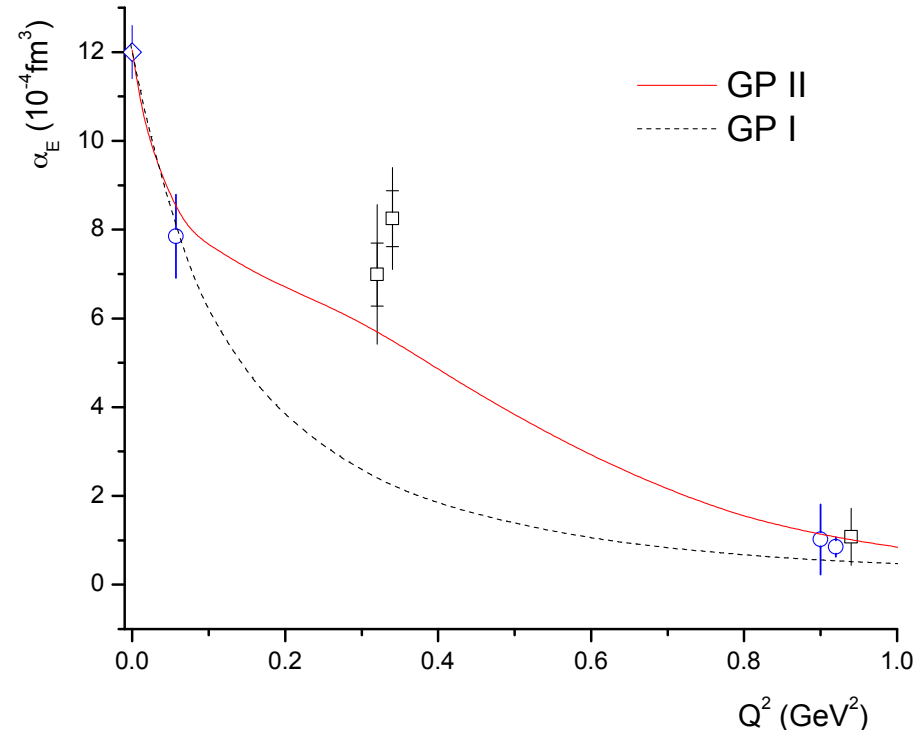
Light (dark) regions → largest (smallest) values
(photon polarization along x-axis, as indicated)



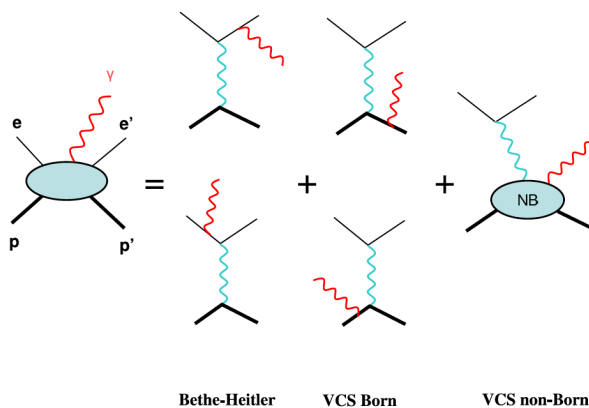
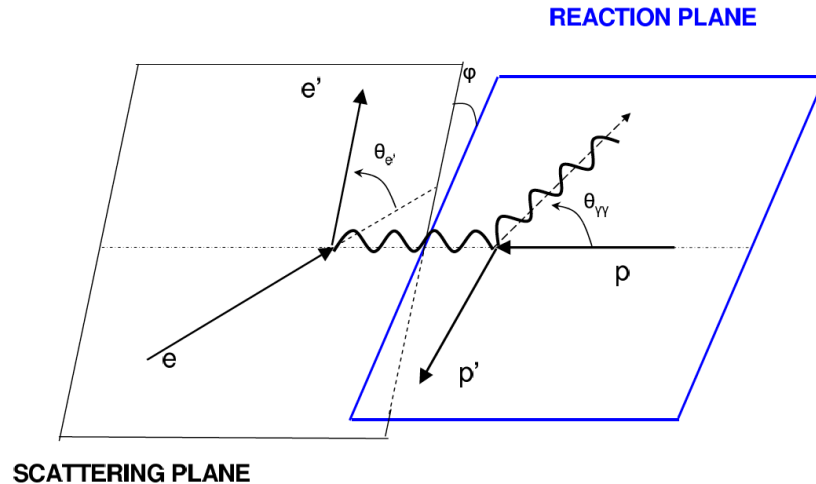
Induced polarization along $b_y = 0$

Phys. Rev. Lett. 104, 112001 (2010)

M. Gorchtein, C. Lorce, B. Pasquini, M. Vanderhaeghen



Virtual Compton Scattering

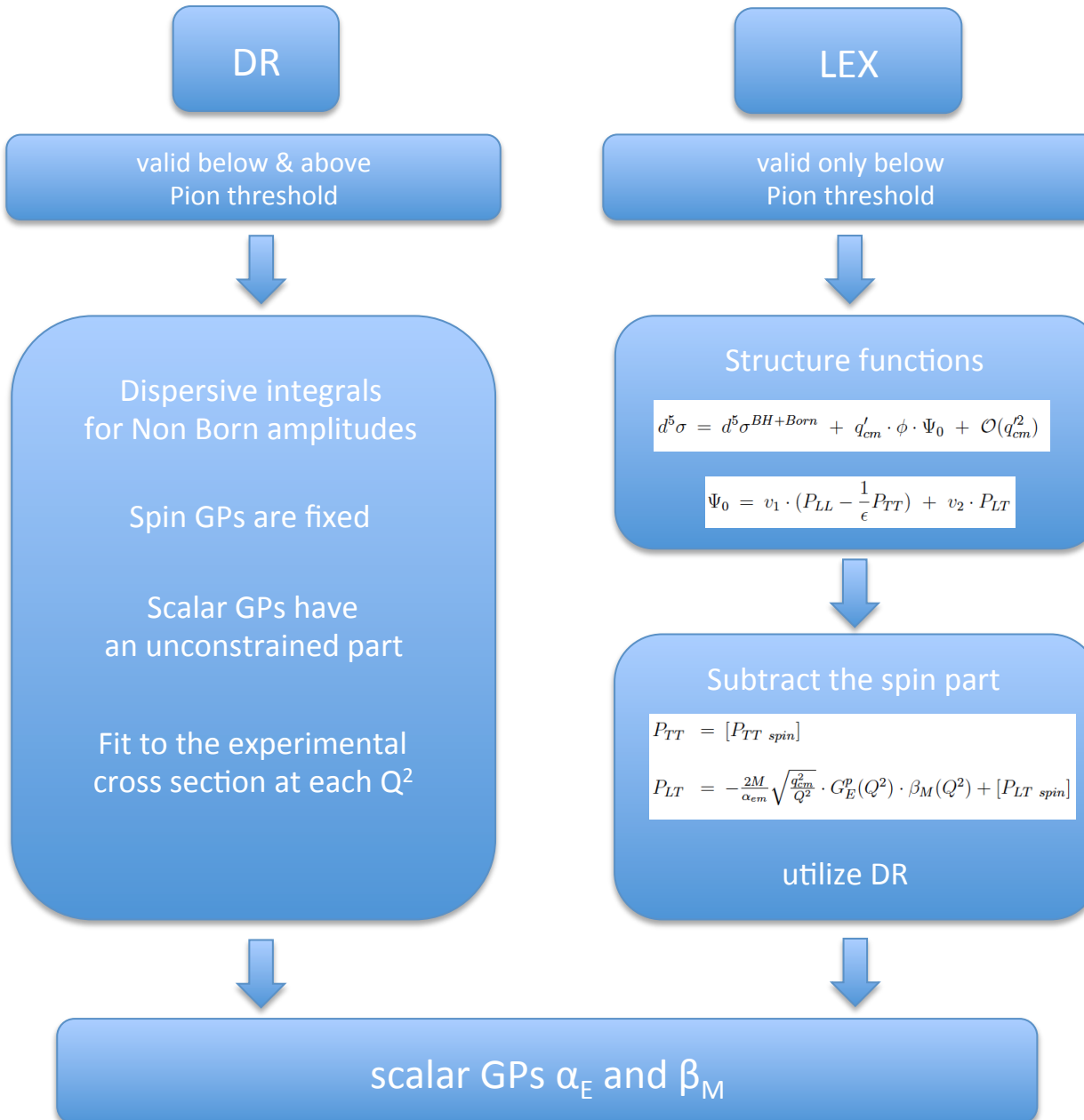


Bethe-Heitler VCS Born VCS non-Born

Elastic FFs

GPs

Virtual Compton Scattering



Virtual Compton Scattering

For LEX the higher order terms have to be negligible

$$d^5\sigma = d^5\sigma^{BH+Born} + q'_{cm} \cdot \phi \cdot \Psi_0 + \mathcal{O}(q'^2_{cm})$$

A phase space masking has to be applied to keep these terms smaller than the 2%-3% level

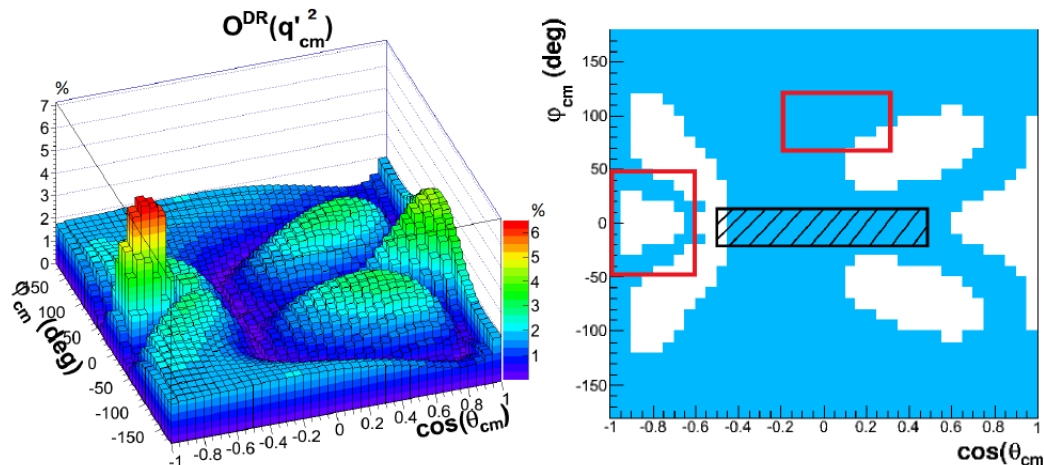


Figure 3.13: (Left) behavior of $\mathcal{O}^{DR}(q'_{cm})^2$ in the $(\cos(\theta_{cm}), \varphi_{cm})$ -plane at $q'_{cm} = 87.5 \text{ MeV}/c$ and (right) two-dimensional representation of the angular region where $\mathcal{O}^{DR}(q'_{cm})^2 < 2\%$ (blue), the red squares correspond to the two areas of interest to perform the GP extraction.

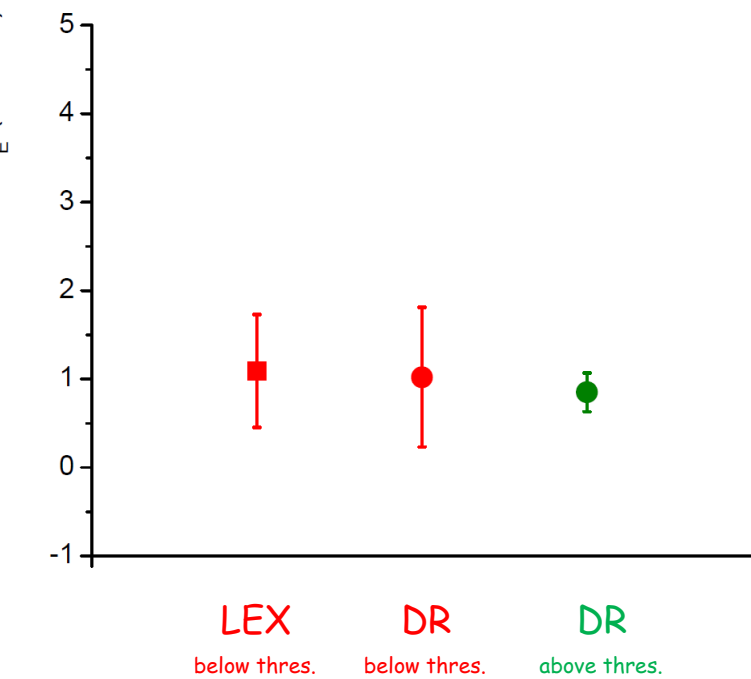
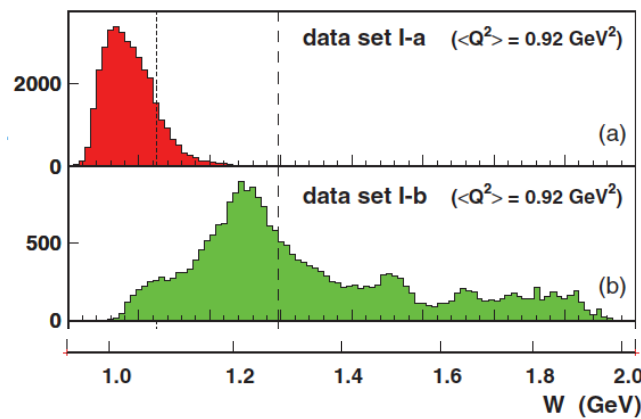
Figure from PhD thesis of L. Correa, Mainz / Cl. Ferrand, 2016

Virtual Compton Scattering

LEX vs DR

Phys. Rev C 86, 015210 (2012)

Phys. Rev Lett. 93, 122001 (2004)



Sensitivity to the GPs grows with the photon energy

Ongoing Experimental Efforts

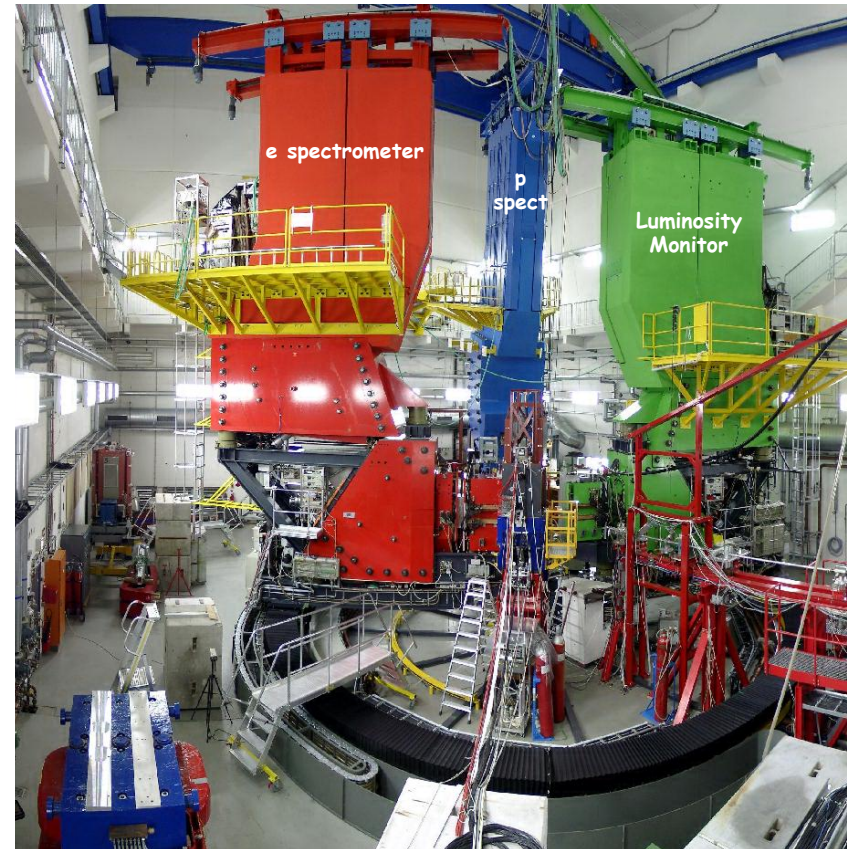
MAMI A1/1-09 (vcsq2) Fonvieille et al below threshold

MAMI A1/3-12 (vcsdelta) Sparveris et al above threshold

Both experiments utilized
the A1 setup at MAMI

Preliminary results were
recently released (LEPP 2016)

Analysis is ongoing



Ongoing Experimental Efforts

vcsq2 @ MAMI

$\sim 1.0 \text{ GeV}$ beam

$Q^2 = 0.1 \text{ (GeV/c)}^2, 0.2 \text{ (GeV/c)}^2, \text{ and } 0.45 \text{ (GeV/c)}^2$

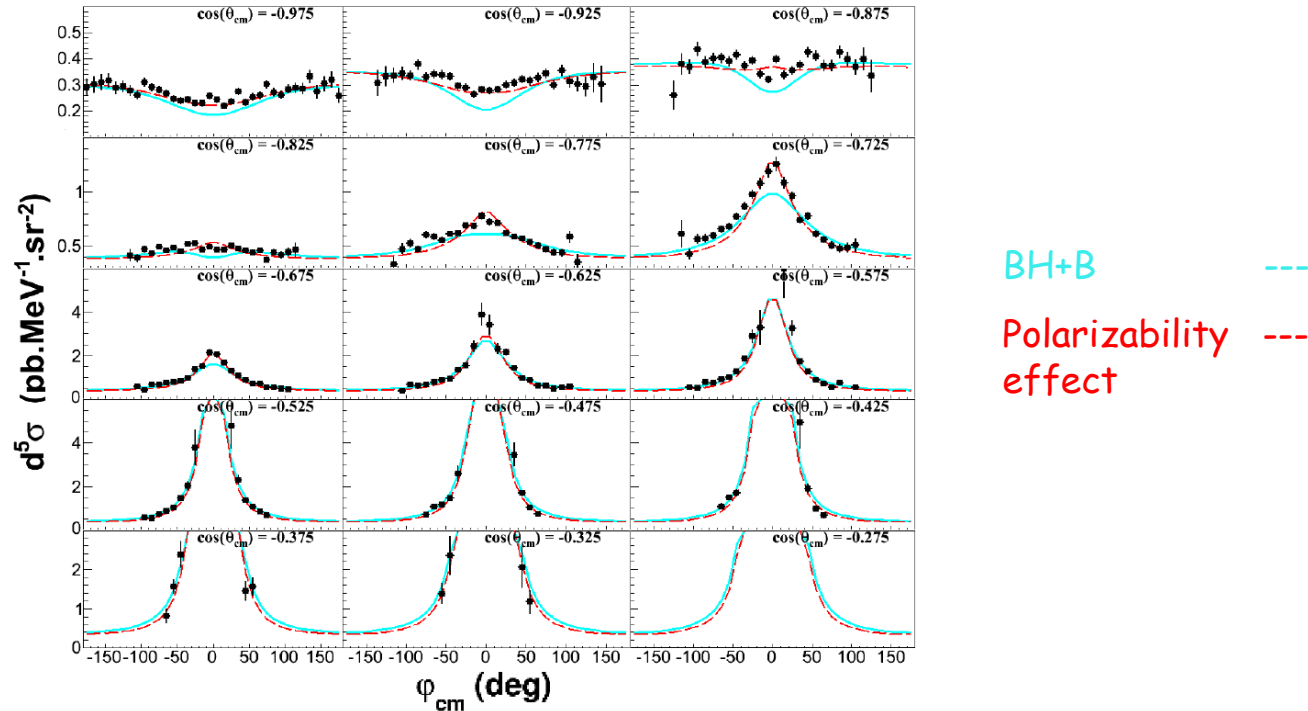


Figure 5.8: Setting INP: measured $ep \rightarrow epi\gamma$ cross section at fixed $q'_{cm} = 112.5 \text{ MeV}/c$ with respect to φ_{cm} for all the $\cos(\theta_{cm})$ -bins. The curves follow the convention of figure 5.6.

Figure from PhD thesis of L. Correa, Mainz / Cl. Ferrand, 2016

Ongoing Experimental Efforts

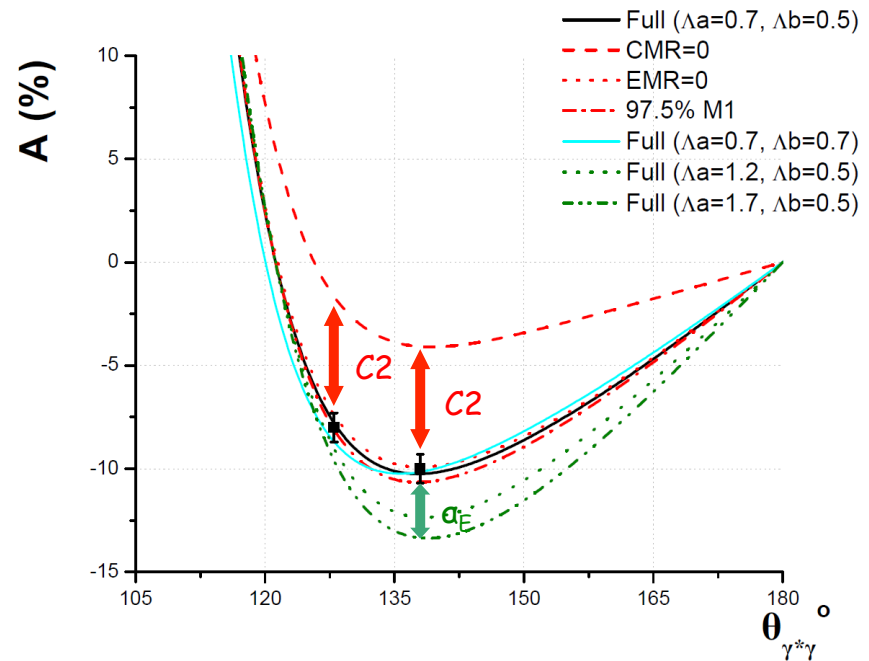
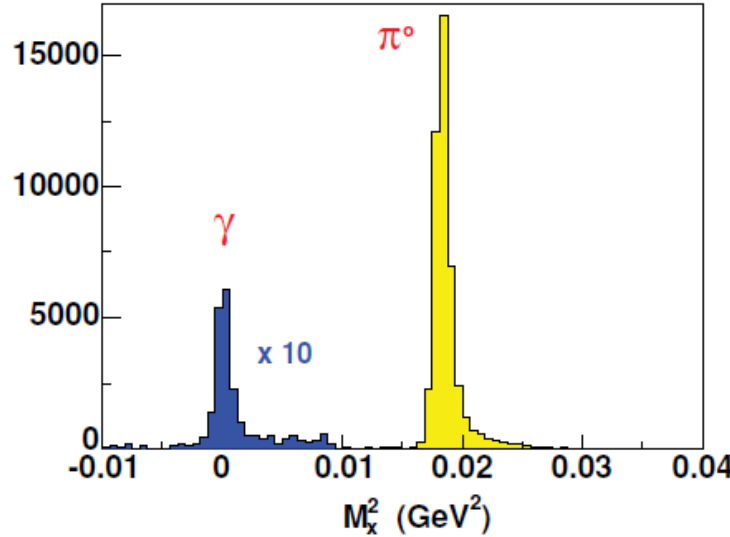
vcsdelta @ MAMI

Data taken in fall 2012

1.1 GeV beam at 30 μA 5cm LH2 250 hrs of beam time

Measurement at $Q^2 = 0.2 \text{ (GeV/c)}^2$

- Goal 2-fold:
- 1) Measurement of the electric GP a_E
 - 2) First measurement of $N \rightarrow \Delta$ transition form factors through the γ channel



Ongoing Experimental Efforts

MAMI A1/1-09 Fonvieille et al

VCS below threshold

data analysis ongoing

MAMI A1/3-12 Sparveris et al

VCS above threshold

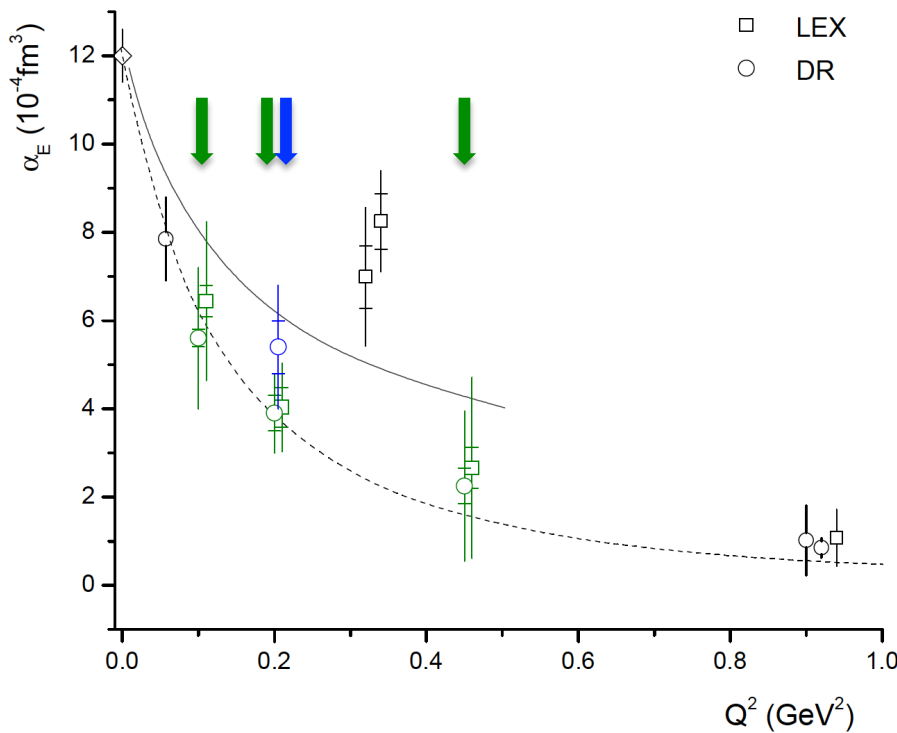
data analysis ongoing

new MAMI measurements competitive to the $Q^2=0.33 \text{ (GeV/c)}^2$ measurements

MAMI constraints $Q^2 < 0.45 \text{ (GeV/c)}^2$

Preliminary A1/1-09 (vcsq2)

Preliminary A1/3-12 (vcsdelta)



Preliminary results:

LEPP conference, Mainz, April 2016

Clermont-Fd & Temple groups

4 PhD students

2 independent measurements at $Q^2=0.20 \text{ (GeV}^2)$

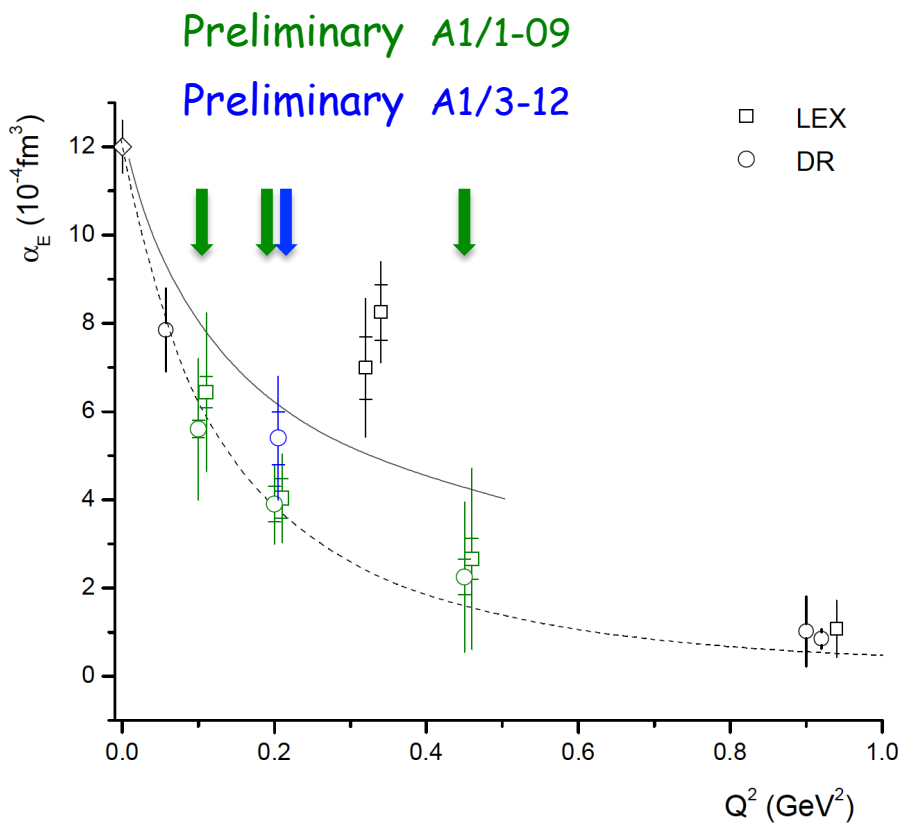
Revisiting the $Q^2=0.33 \text{ (GeV}/c)^2$ measurements

$Q^2 = 0.33 \text{ (GeV}/c)^2$ measured twice at MAMI

Two different experiments - a few years apart

- Phys. Rev. Lett 85, 708 (2000)
- Eur. Phys. J. A37, 1-8 (2008)

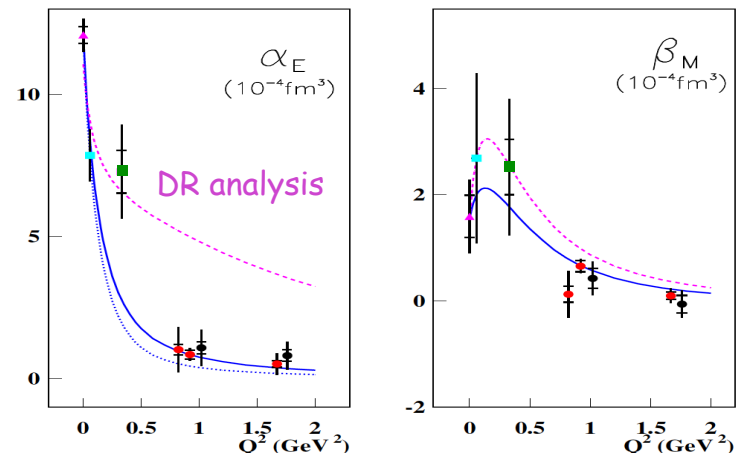
Results from both experiments through LEX



DR analysis of the data:

Eur. Phys. J A 28, s1, 117 (2006)

DR - LEX agreement



DR & LEX analysis recently revisited

Currently ongoing effort

Results so far still point out to an enhanced α_E value at $Q^2=0.33 \text{ (GeV}/c)^2$

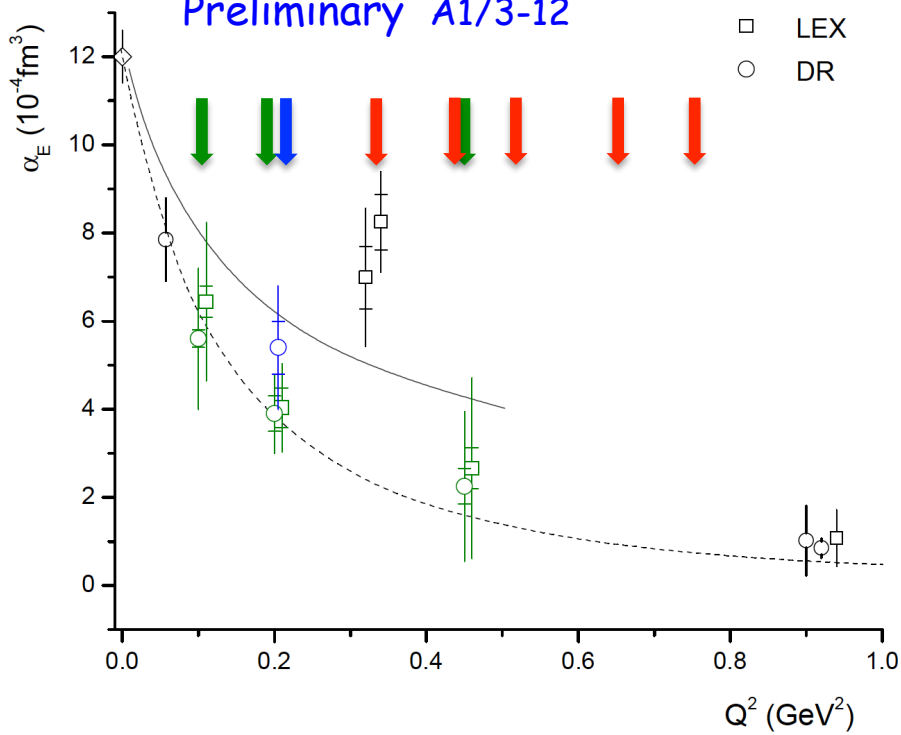
Ongoing Experimental Efforts

JLab

E12-15-001
(JLab)

Preliminary A1/1-09

Preliminary A1/3-12



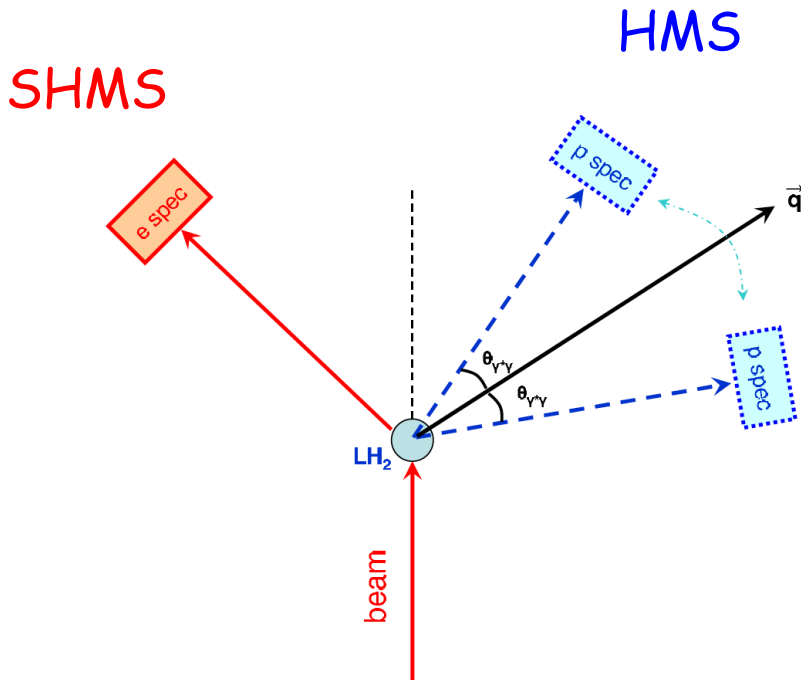
Will double the sensitivity to the GPs

additional + :

Beam energy $\times 4$

Beam current $\times 5$

E12-15-001 Experimental Setup



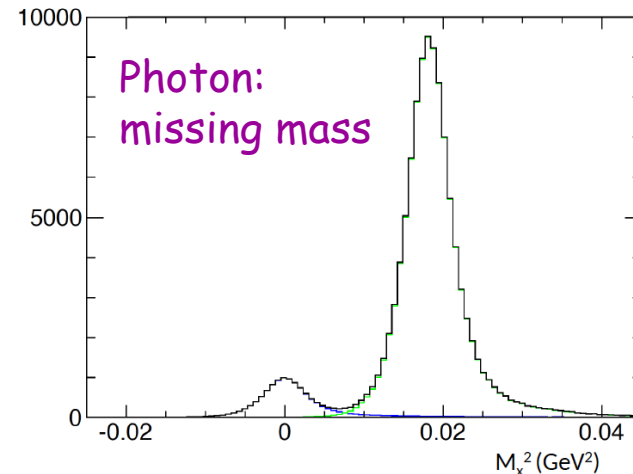
Hall C: SHMS, HMS

4.4 GeV

40-85 μ A

Liquid hydrogen 15 cm

e & p detection in coincidence



cross sections

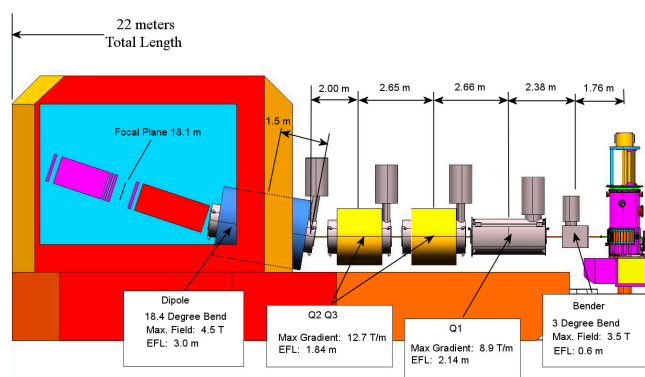
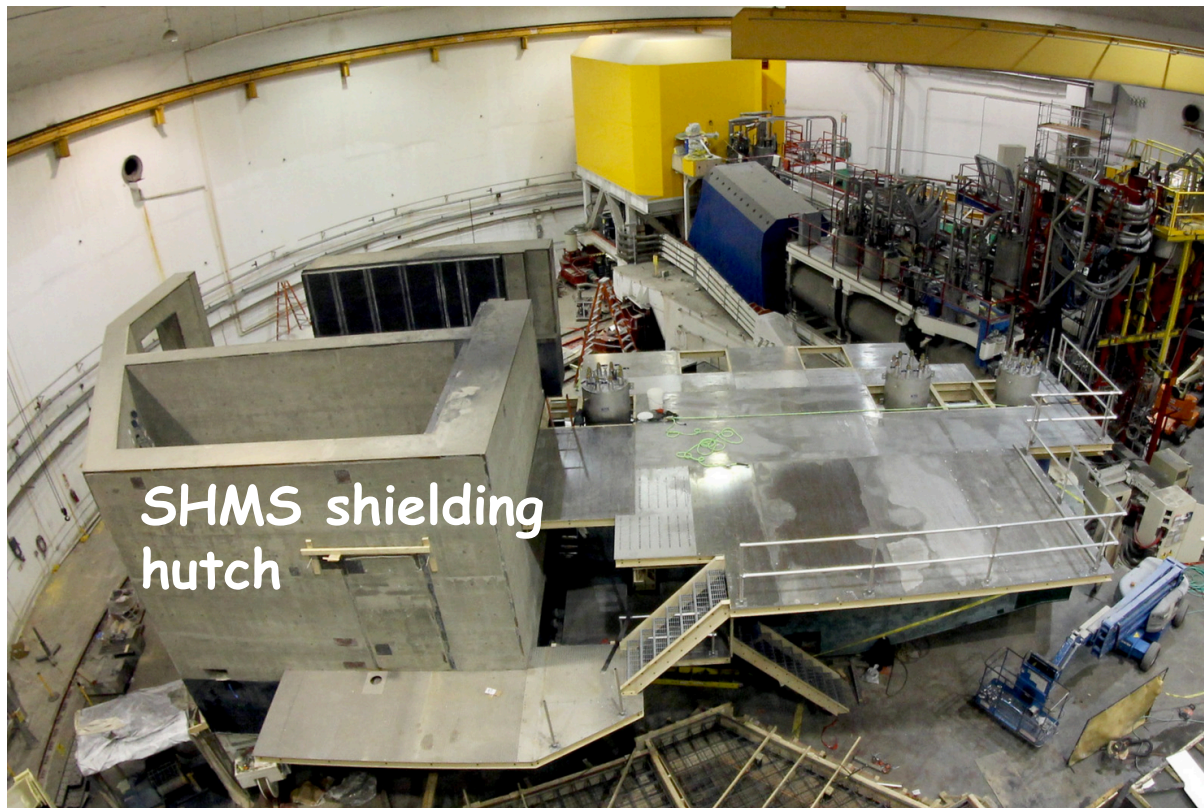
in-plane azimuthal asymmetries

$$A_{(\phi_{\gamma^*\gamma}=0,\pi)} = \frac{\sigma_{\phi_{\gamma^*\gamma}=0} - \sigma_{\phi_{\gamma^*\gamma}=180}}{\sigma_{\phi_{\gamma^*\gamma}=0} + \sigma_{\phi_{\gamma^*\gamma}=180}}$$

sensitivity to GPs

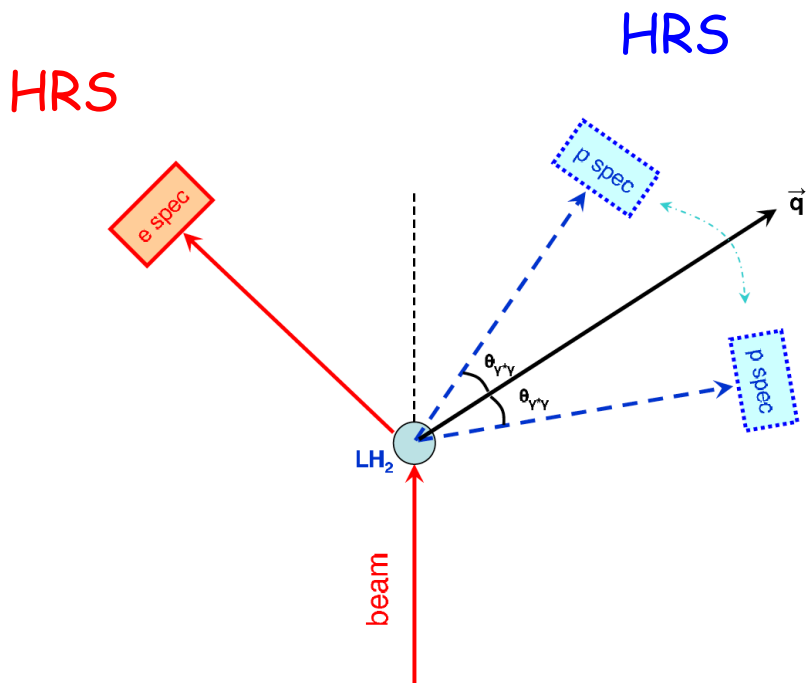
suppression of systematic asymmetries

Hall C Overview



SHMS

Alternative Experimental Setup



Hall A (?)

HRS min. angle = 12.5 deg

Can not run Part I with 4.4 GeV

Run Part I with a lower beam energy

Part I with 3.3 GeV:

- Reduced sensitivity to GPs
 - Smaller cross section
- $\delta\alpha_E$ increased by 16.5%

(still very competitive measurement)

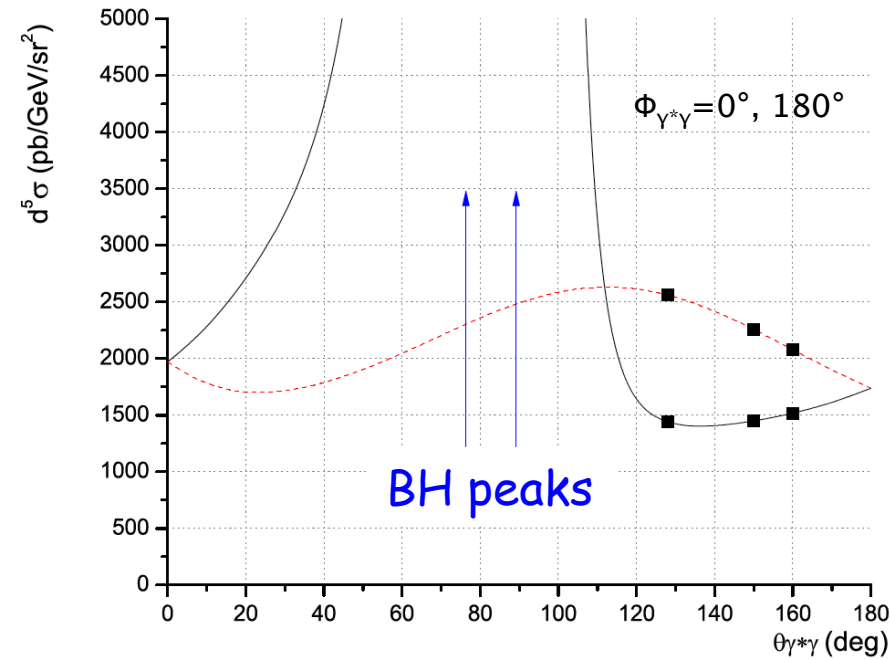
Hall A: HRS(e), HRS(p)
3.3 GeV 6.5 days
4.4 GeV 10.5 days

Will not be able to allow for the maximum beam energy to another Hall during Part I (6.5 days)

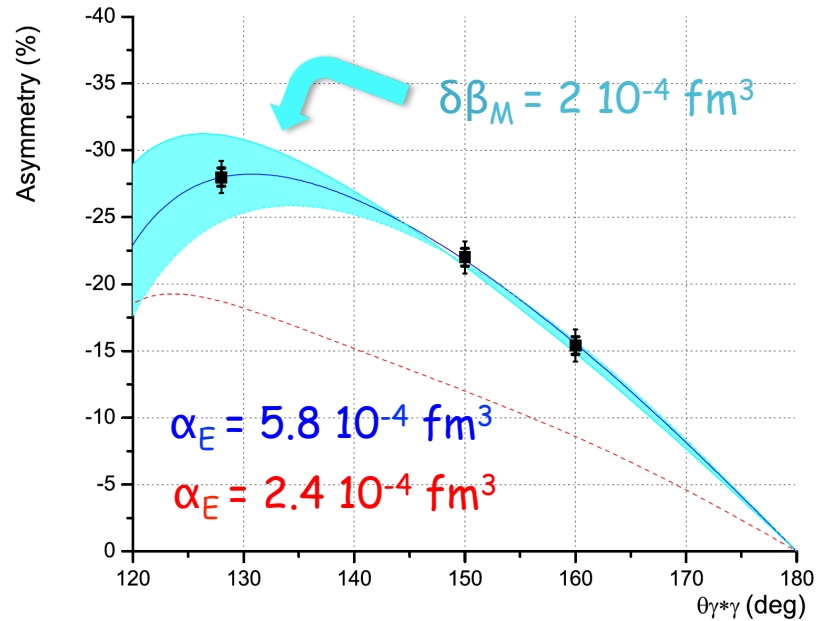
The high Q^2 Jlab measurements (E93-050) were done in Hall A with the two HRSs, a 15 cm LH₂ target, and a 4 GeV beam

Projected Measurements

$$Q^2 = 0.43 \text{ (GeV/c)}^2$$



avoid BH peaks
stay at $\theta_{\gamma^*\gamma} > 120^\circ$



Kinematical Settings

	Kinematical Setting	$\theta_{\gamma^*\gamma} \circ$	$\theta_e \circ$	$P'_e(MeV/c)$	$\theta_p \circ$	$P'_p(MeV/c)$	S/N	beam time (days)
Part I	Kin Ia	155	7.97	3884.4	37.20	893.20	1.1	0.5
	Kin Ib	155	7.97	3884.4	51.26	893.20	2.7	0.5
	Kin IIa	140	7.97	3884.4	33.08	859.90	1	0.45
	Kin IIb	140	7.97	3884.4	55.38	859.90	3.7	0.55
	Kin IIIa	120	7.97	3884.4	27.85	794.68	0.9	0.45
	Kin IIIb	120	7.97	3884.4	60.61	794.68	6.2	0.55
	Kin IVa	165	9.39	3820.5	40.85	1010.40	1.3	0.5
	Kin IVb	165	9.39	3820.5	48.45	1010.40	2.4	0.5
	Kin Va	155	9.39	3820.5	38.34	995.20	1	0.5
	Kin Vb	155	9.39	3820.5	50.96	995.20	3.2	0.5
Part II	Kin VIa	128	9.39	3820.5	31.84	919.43	0.7	0.95
	Kin VIb	128	9.39	3820.5	57.46	919.43	7.8	0.55
	Kin VIIa	165	11.54	3708.6	40.81	1175.25	2.6	1.5
	Kin VIIb	165	11.54	3708.6	47.35	1175.25	5	2
	Kin VIIIa	160	11.54	3708.6	39.73	1167.72	2.2	1.5
	Kin VIIIb	160	11.54	3708.6	48.43	1167.72	6.3	2
Part II	Kin IXa	140	11.54	3708.6	35.52	1117.38	1.2	1.5
	Kin IXb	140	11.54	3708.6	52.64	1117.38	8	2

Part I

Part II

SHMS: one change of setting through Part I
same position & momentum through out Part II

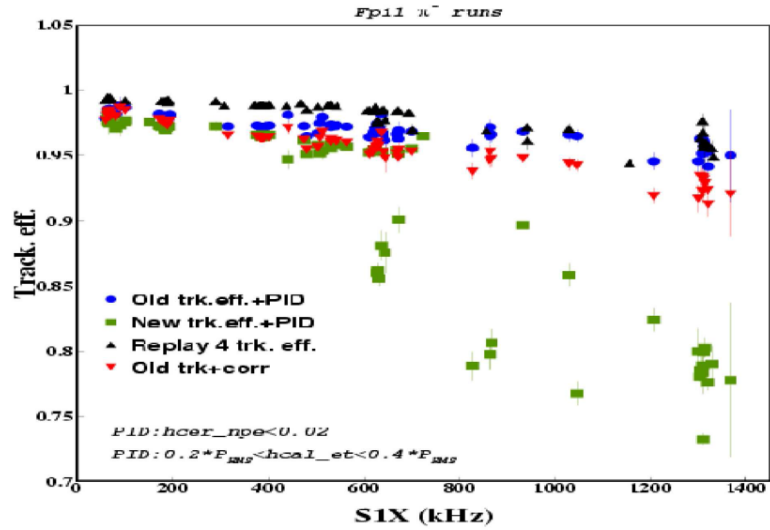
Part	I	I	I	II	II
Q ²	0.33 (GeV/c) ²	0.43 (GeV/c) ²	0.52 (GeV/c) ²	0.65 (GeV/c) ²	0.75 (GeV/c) ²

Kinematical Settings

HMS singles rates

	Kinematical Setting	HMS singles rates (kHz)
Part I	Kin Ia	163
	Kin Ib	43
	Kin IIa	244
	Kin IIb	31
	Kin IIIa	300
	Kin IIIb	21
	Kin IVa	213
	Kin IVb	91
	Kin Va	290
	Kin Vb	68
	Kin VIa	300
	Kin VIb	34
Part II	Kin VIIa	102
	Kin VIIb	37
	Kin VIIIa	122
	Kin VIIIb	31
	Kin IXa	244
	Kin IXb	16

HMS Tracking Efficiency



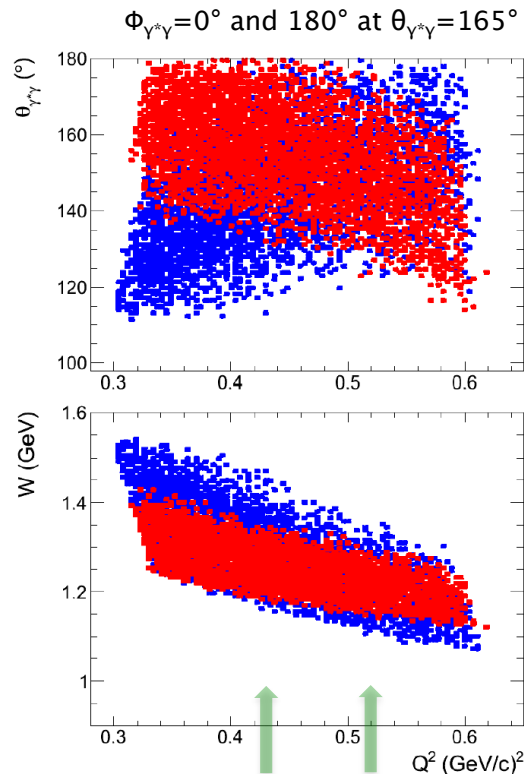
HMS singles rates kept below 300 kHz

Kin I, I, III, VIa → 40 - 50 μ A

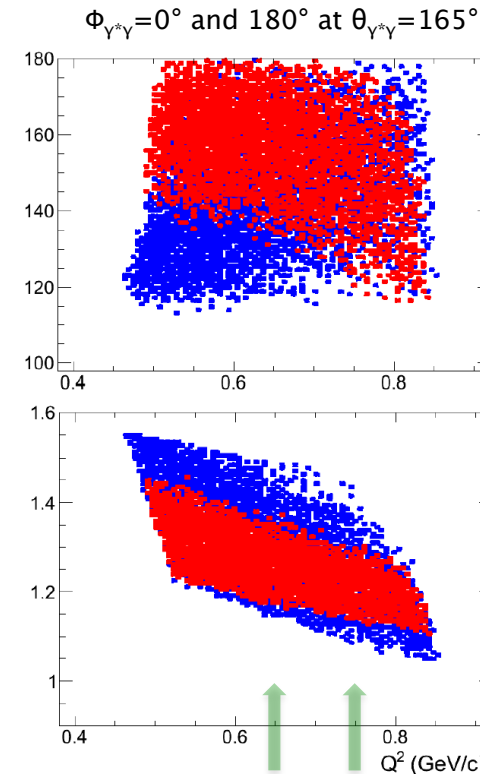
All other settings → 85 μ A

Phase Space

Part I



Part II



Phase space binned
in Q^2 , W , $\theta_{\gamma^*\gamma}$, $\Phi_{\gamma^*\gamma}$

Cross section:
DR calculation,
B. Pasquini

Eur. Phys. J. A11 (2001) 185-208
Phys. Rept. 378 (2003) 99-205

Part

I

I

I

II

II

Q^2

0.33 (GeV/c)

0.43 (GeV/c^2)

0.52 (GeV/c^2)

0.65 (GeV/c^2)

0.75 (GeV/c^2)

Measurements

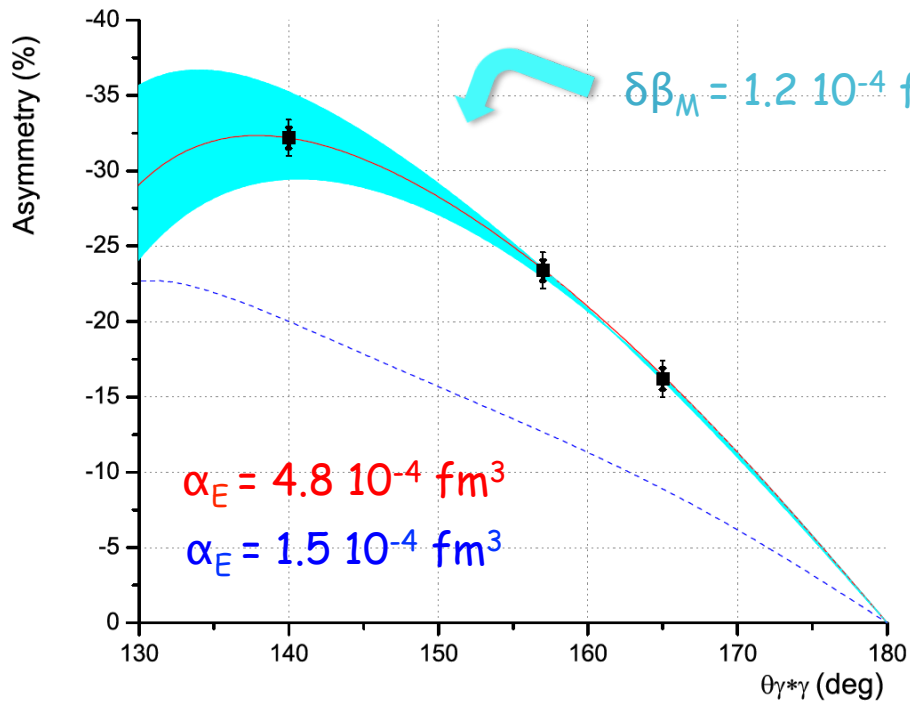
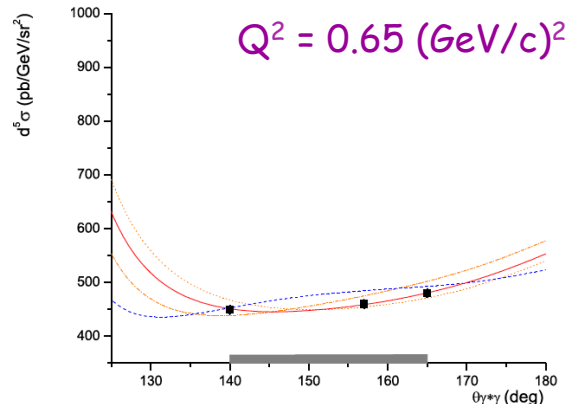
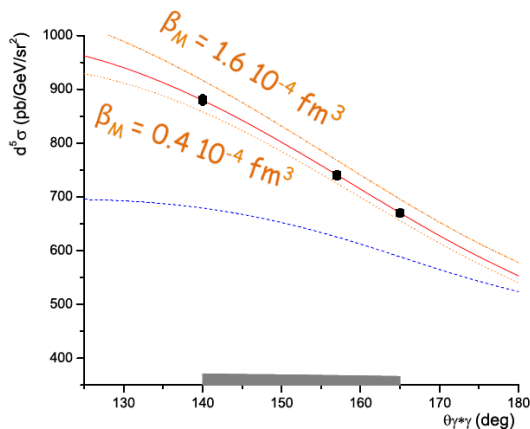
Plus for systematics:

- Electron momentum & angle: one change during Part I
- Electron momentum & angle stays fixed through out Part II
- Proton momentum stays fixed for the asymmetry pair ($\Phi_{\gamma^*\gamma} = 0^\circ, 180^\circ$) measurements
- No beam energy changes

$p(e,e'p)\pi^0$ measured for free

- High statistics
- Cross section very well known in this region
- Additional normalization per setting

Measurements

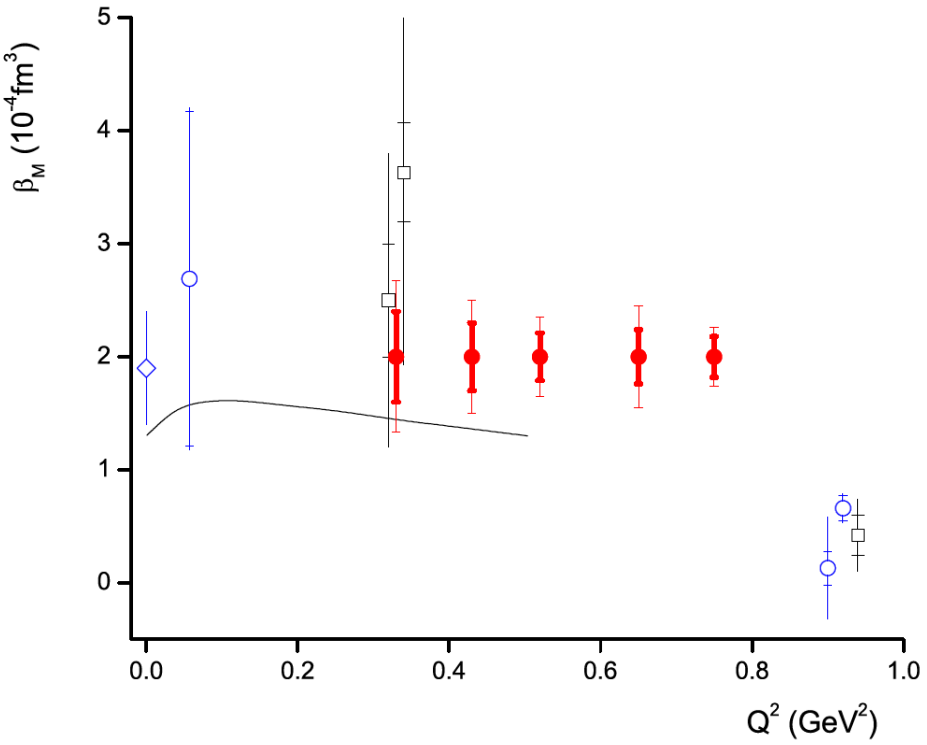
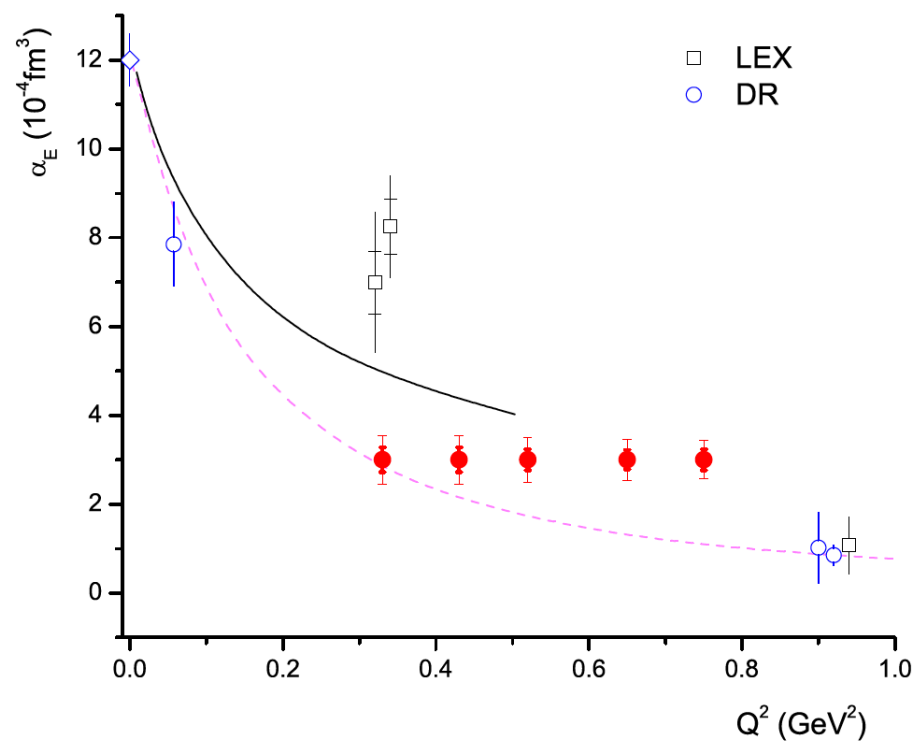


Statistical	< ±1.3%
Beam energy / scat. Angle	±1-2.5%
Target density	±0.5%
Detector efficiency	±0.5%
Acceptance	±0.5%
Target cell backgr.	±0.5%
Target length	±0.3%
Beam charge	±0.3%
Dead time	±0.3%
Pion contamination in MM	±0.3%
Rad. Corr.	±1.5%
Other	±0.5%

σ < ±1.3% (stat) < ±3.3% (syst)

A ≈ ±0.7% (stat) ≈ ±1.1% (syst)

Projected Measurements

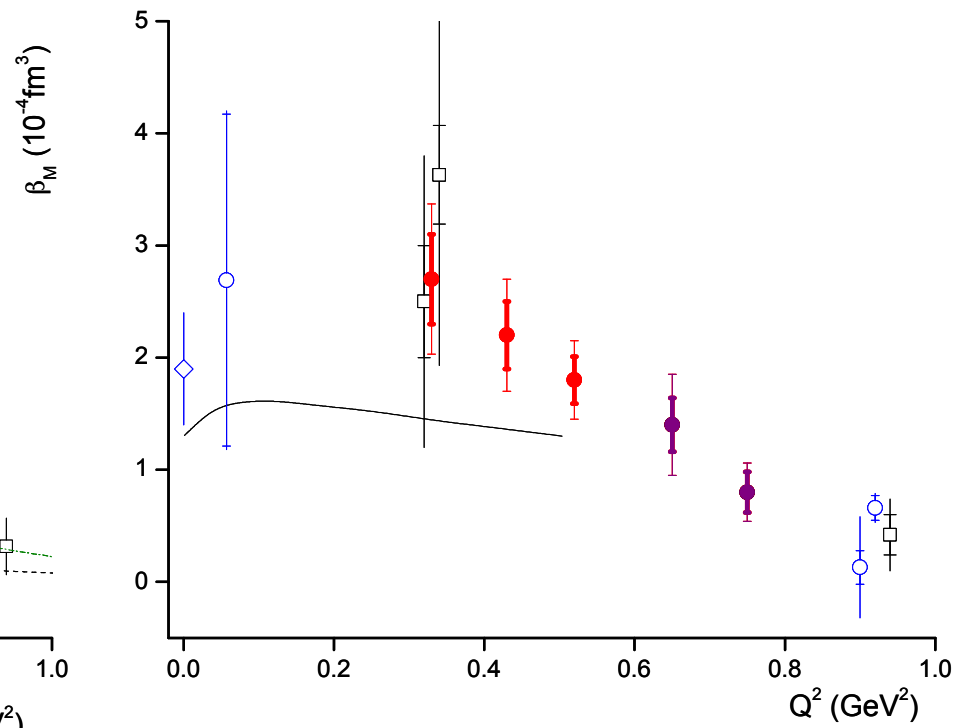
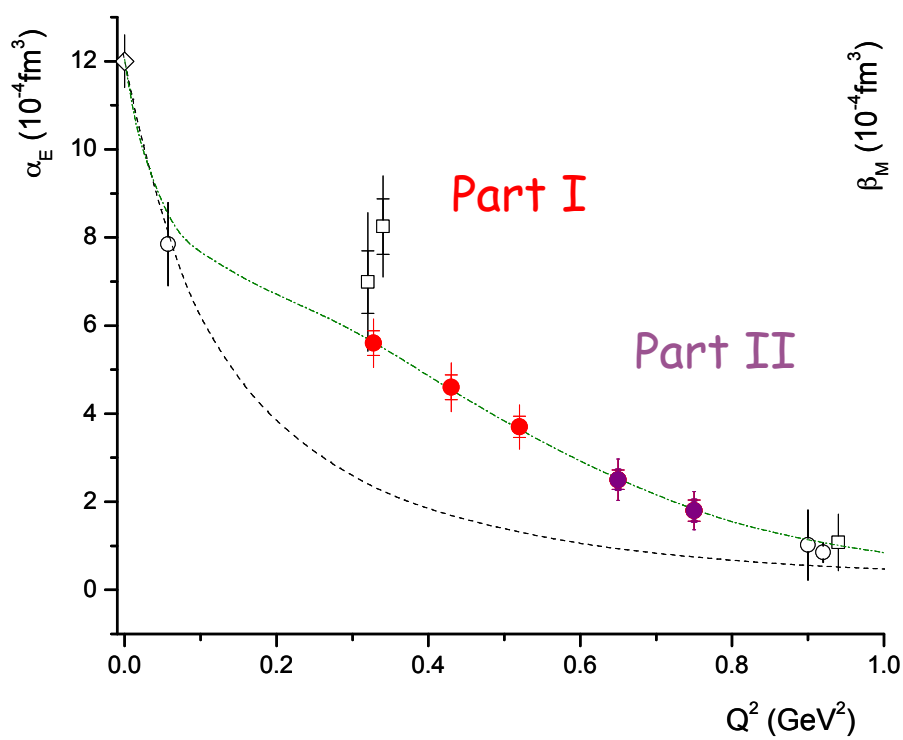


$$\delta_{\text{GPs(stat)}} \approx 0.7 \delta_{\text{GPs(syst)}}$$

$$\delta_{\text{GPs(syst)}} \approx \delta_{\text{GPs(FFs/DRmult)}}$$

Status of E12-15-001

(arbitrarily projected points)



Part I approved in summer 2016 (Jlab PAC 44): $(4.4 \text{ GeV}, 85 \mu\text{A}, \text{Hall C})$

Scheduling request will be submitted in spring 2017

Beamtime request for Part II will follow the first results of Part I

Summary

Electric and Magnetic GPs

- fundamental structure constants
- internal structure and dynamics of the nucleon
- complementary to elastic & transition FFs, GPDs, TMDs, ...

Puzzle w.r.t. a_E

New measurements in a region very sensitive to the nucleon dynamics

- moving towards improving the precision of a_E and β_M by a factor of 2
- high precision mapping vs Q^2 - cross check of measurements from different labs
- explore non trivial Q^2 dependence of a_E (mesonic cloud, something else ... ?)
- quantify the balance between paramagnetism and diamagnetism through β_M
- provide, with high precision, the spatial deformation of charge & magnetization densities under an applied e.m. field (currently a profound structure is suggested in the region 0.5 fm - 1 fm)
- Lattice QCD results will be emerging in the next few years - very important to cross check these calculations
- the new measurements will trigger more theoretical activity

Thank you!